Modelling the Quantum Capacitance of Single-layer and Bilayer Graphene

Yousra AMMOUR [1, 2] *, Riad REMMOUCHE [1, 2], Rachid FATES [2]

[1] *LEM Laboratory, University of Jijel, 18000 Jijel, Algeria*
[2] *Faculty of Science and Technology, University of Jijel, 18000 Jijel, Algeria*

In this paper, we report the modelling of quantum capacitance in both single-layer and bilayer graphene devices to investigate the temperature dependence. The model includes the existence of electron and hole puddles due to local fluctuations of the potential, which is taken into account with the possibility of finite lifetimes of electronic states to calculate the quantum capacitance using the Gaussian distribution. The results indicate that the simulations are in agreement with the experimental measurements, which proves the accuracy of the proposed model. On the other hand, temperature dependence around the charge neutrality point has been reported for both single and bilayer graphene.

Keywords: graphene, temperature, electron-hole puddles, doping, charged impurities.

1. INTRODUCTION

Graphene is a single-layer of two-dimensional carbon atoms that was discovered in 2004 [1]. It has received much attention in recent years because of its extraordinary properties [2], including excellent transport properties expressed by high charge carrier mobility. There is the possibility of tuning the ultra-high mobility by introducing anti-site defects in the single-layer [3], which makes this material attractive for high-speed electronics [4].

Bilayer graphene has the property of controlling both carrier density and band gap by applying gate bias [5] or doping [6], which makes it a serious candidate for a wide range of applications [7, 8]. The band structure near the Dirac point represents the main parameter to distinguish the two types of single-layer and bilayer graphene. Single-layer graphene exhibits a conical band structure and a density of states that linearly disappears at the Dirac point. The latter, which is the epicentre of the Dirac cone that describe the electronic structure of 2D material, is a key parameter that provides several information, especially the doping properties. In contrast, bilayer graphene exhibits a low-energy parabolic band structure and a density of states that increases linearly with energy from a finite value at zero energy [9], as results, the quasi-particles in bilayers are chiral massive fermions that differ from those in single-layer (massless fermions) [10].

One major application of this material is as a channel for field-effect transistors (FETs), where a sample is placed on an oxidized silicon substrate and connected to source and drain electrodes. Generally, it is well known that the dominant capacitance in this configuration is the oxide capacitance, however because of the scale of graphene devices, the quantum capacitance becomes dominant [11].

Several theoretical and experimental studies [12, 13] have reported the determination of the quantum capacitance of graphene. Despite the fact that graphene-based materials are still undergo study due to the low density of free electrons. It has been noted that the quantum capacitance of these materials plays an important role when they are used as electrode materials. To our knowledge, from the theoretical work of the literature, the quantum capacitance of graphene is the limiting factor influencing the total capacitance [14]. Unlike in the conventional 2D systems, the density of states in graphene depends on doping, this makes even small density of states contributions readily noticeable to the structure/device geometrical capacitance. This allowed observations of graphene's quantum compressibility. Likewise, considerable charge inhomogeneity typical for graphene deposited on silicon oxide leads to strong spatial averaging. This inhomogeneity obscures details in the DoS which can indicate new phenomena in relationship with quantum capacitance [15]. So, this parameter is important for understanding fundamental electronic properties of the material such as the density of state, also it gives graphene an advantage in sensing applications [16]. Here, we present a simple analytical model for the quantum capacitance of both single-layer and bilayer graphene devices. This model takes into account the electron-hole puddles induced by charged impurities and possibly finite lifetimes of electro-nic states through a Gaussian broadening distribution as well as the energy broadening parameter with a value of $E_{br} = 75$ MeV. The temperature dependence of the quantum capacitance as a function of the Fermi level for a graphene-based device single-layer and bilayer is investigated.

2. MODEL DESCRIPTION

2.1. Single-layer graphene

To determine the quantum capacitance, the existence of electron and hole puddles has been considered to include both single and bi-layer graphene. As reported by Fates et al. [9], for single-layer graphene (SLG), the electrons have a relativistic zero mass fermions behavior. Physically, both

---

the Hamiltonian and the susceptibility can be decomposed into those equivalent to the monolayer band. The monolayerlike band exists only in odd-layered graphenes and gives a strong diamagnetic peak at zero energy [17]. These electrons obey the following linear dispersion relation [18]:

$$\chi(k) = \pm\left(\hbar v_F \, |k|\right), \tag{1}$$

where (+) corresponds to the conduction band and (-) corresponds to the valence band, $\hbar$ is the reduced Plank constant, $v_F \sim 10^6$ m/s is the Fermi velocity of the charge carriers in graphene, and k represents the wave vector in the 2D plane of the graphene sheet which is expressed as $|k| = (k_x^2 + k_y^2)^{0.5}$. When $k = 0$, the energy at the Dirac point $\varepsilon(k=0) = 0$ eV could be a convenient choice for the energy reference.

In an undoped single-layer graphene (SLG) in the thermal equilibrium state, electrons and holes are created in the conduction band and valence band respectively. The linear density of states (DOS) of SLG is given by [19]:

$$DOS_{SLG}(\chi) = \frac{2|\chi|}{\pi(\hbar v_F)^2} . \tag{2}$$

When the graphene is deposited on a substrate, there are various defects and charged impurities that contribute to the creation of electron/hole puddles, which leads to an inhomogeneous distribution of charge carrier density [20]. The broadened density of states that takes into account the electron-hole puddles and the possible finite lifetime of the electronic states through a Gaussian broadening distribution is expressed as follows [21]:

$$D(\chi) = \frac{1}{\sqrt{2\pi}E_{br}} \int_{-\infty}^{+\infty} \exp\left(-\frac{(\eta-\chi)^2}{2E_{br}^2}\right) DOS(\eta)\, d\eta, \tag{3}$$

where E_{br} is the energy broadening parameter. From the integration of Eq. 3, we obtain the broadened density of states for SLG:

$$D_{SLG}(\chi) = \frac{2}{\pi(\hbar v_F)^2}\left[\frac{2E_{br}}{\sqrt{2\pi}}\exp\left(-\frac{\chi^2}{2E_{br}^2}\right) + \chi\, erf\left(\frac{\chi}{E_{br}\sqrt{2}}\right)\right] \tag{4}$$

As reported in the literature, the quantum capacitance depends on the density of states in the channel [22]. On the other hand, using the definition, $C_Q = q(dQ_{tot}/dE_F)$, where $Q_{tot} = q(n-p)$ is the total charge density in a graphene sheet corresponding to the local electrostatic potential and the Fermi energy, i.e. $qV_{ch} = E_F$, we obtain :

$$C_Q(E_F) = C_0\left[\left(erf\left(\frac{\chi_2}{E_{br}\sqrt{2}}\right) - erf\left(\frac{\chi_1}{E_{br}\sqrt{2}}\right) - 2\right) \times \left(\ln\left(1+e^{\alpha E_F/KT}\right) - \ln\left(1+e^{-\alpha E_F/KT}\right)\right)\right], \tag{5}$$

where K is the Boltzmann constant, T is the temperature, $C_0 = 2q^2/\pi(\hbar v_F)^2$ is the dimensional unit of C_Q the quantum capacitance, $erf(\chi)$ is the Gaussian error function and α is the fitting parameter. Note that χ_1 and χ_2 are mathematical parameters tending to $-\infty$ and $+\infty$ for hole and electron respectively.

2.2. Bilayer graphene

Unlike SLG which has a density of states that disappears linearly at the Dirac point, bilayer graphene (BLG) has a quite constant density of states near the Dirac point due to parabolic dispersion [23]. The dispersion relation for bilayer graphene is given by [24]:

$$\chi(k) = \pm\left(\mu\frac{t_1}{2} + \sqrt{\left(\frac{t_1}{2}\right)^2 + (\hbar v_F k)^2}\right), \tag{6}$$

where the parameter μ toggles between -1 and +1. For the negative value of μ, both bands are closer to zero energy, elsewhere the two bands are repulsed by t_1 which represents the vertical coupling between the two atoms in the Bernal configuration. The density of states of pure and perfect bilayer graphene can be approximated in the range of energy $|\varepsilon| \le t_1$ by a linear relationship as a function of energy [26] as follows:

$$DOS_{BLG}(\chi) = \frac{2}{\pi(\hbar v_F)^2}\left(|\chi| + \frac{t_1}{2}\right) \tag{7}$$

By integrating Eq. 3, we get the broadened density of states for the BLG:

$$D_{BLG}(\chi) = \frac{2}{\pi(\hbar v_F)^2}\left[\frac{2E_{br}}{\sqrt{2\pi}}\exp\left(-\frac{\chi^2}{2E_{br}^2}\right)\right.$$
$$\left. + \chi\, erf\left(\frac{\chi}{E_{br}\sqrt{2}}\right) + \frac{t_1}{2}\right] \tag{8}$$

As carried out for SLG, the BLG quantum capacitance expression can be extracted as follows:

$$C_Q(E_F) = C_0\left[\frac{KT}{2}\left(erf\left(\frac{\chi_2}{E_{br}\sqrt{2}}\right) - erf\left(\frac{\chi_1}{E_{br}\sqrt{2}}\right) - 2\right)\right.$$
$$\times\left(\ln\left(1+e^{\alpha E_F/KT}\right) - \ln\left(1+e^{-\alpha E_F/KT}\right)\right) + \frac{t_1}{2}\left(-\frac{1}{1+e^{\frac{\chi_2-\alpha E_F}{KT}}}\right.$$
$$\left.\left. + \frac{1}{1+e^{\frac{\chi_2+\alpha E_F}{KT}}} + \frac{1}{1+e^{\frac{\chi_1-\alpha E_F}{KT}}} - \frac{1}{1+e^{\frac{\chi_1+\alpha E_F}{KT}}}\right)\right]. \tag{9}$$

3. RESULTS AND DISCUSSION

In Fig. 1, we plot the dependence of the quantum capacitance of SLG (Fig. 1 a) and BLG (Fig. 1 b) versus the Fermi level E_F for different values of the temperature.
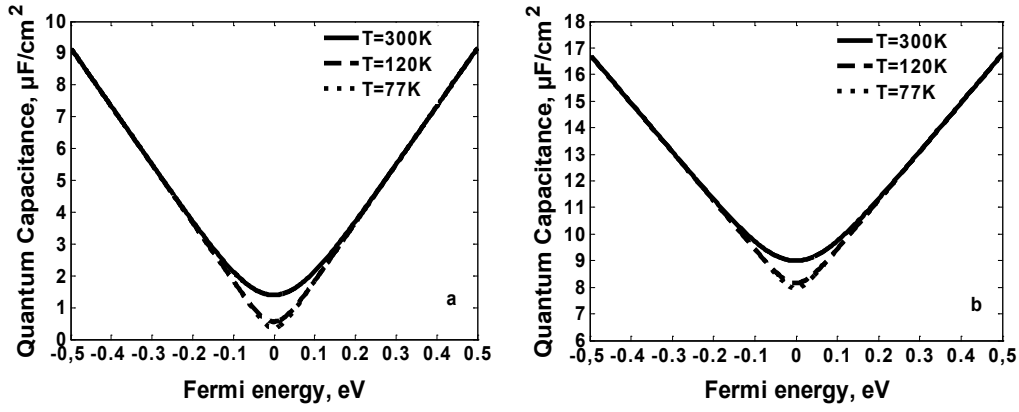
Fig. 1. Quantum capacitance as a function of Fermi level for: a – SLG; b – BLG at several temperature values ranging from 77 K to 300 K. The simulations were performed for E_{br} = 75 MeV and α = 0.47

Our results show that the minimum of the quantum capacitance is reached at the Dirac point. The Dirac point is the access/contact point of the valence band to the conduction band. When the Fermi level converges to the Diract point from the top (bottom), the density of the free electron (hole) decreases. This result means there is a minimum carrier density at the Diract point. The characteristic curvature increases as the temperature decreases. This observation is valid for both SLG and BLG. The quantum capacitance becomes independent of temperature when the Fermi energy keeps rising over E_F = 0.12 eV. This demonstrates the minor effect of the temperature for such Fermi energies. Physically, these results could be explained by the fact that the carriers induced by doping are higher than those induced by temperature beyond E_F = 0.12 eV.

On the other hand, we can distinguish a notable difference between Fig. 1 a and b concerning the quantum capacitance value which varies between 0.2 and 9 µF/cm², and between 8 and 17 µF/cm² for the SLG and BLG respectively. Otherwise, we note a decrease in the minimum value of the quantum capacitance when the temperature goes down for both SLG and BLG. These results are in line with those reported in the literature for both single-layer graphene [13, 16, 18–20, 22, 24, 25, 27] and bi-layer graphene [18, 20, 21, 23, 26, 27].

Fig. 2 shows the comparison between the simulated results and the measured data of the SLG quantum capacitance for three temperature values: 300 K, 120 K and 77 K. The measurements were carried out at the ICTEAM of the Université Catholique de Louvain, Louvain-la-Neuve (Belgium). A good agreement is observed. This allows us to validate the proposed model.

Fig. 3 shows the minimum quantum capacitance $C_{Q, min}$ ratio as a function of temperature. We find a similarity in the temperature dependence of the minimum capacitance of single and bi-layer graphene for low-temperature values, and a difference in the dependence between single and bi-layer graphene for high-temperature values. The large difference in the high-temperature regime between the curves is attributed to the difference that exists in the effect of local potential fluctuations.
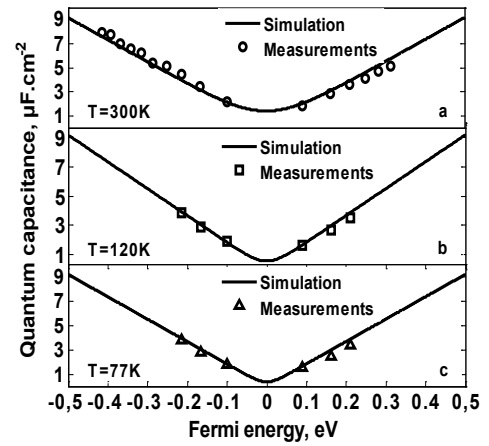

Fig. 2. Temperature dependence of the simulated and measured quantum capacitance as a function of Fermi energy: a – T = 300K, b – T = 120 K and c – T = 77K. The solid lines are the simulations and the symbols are the measurements
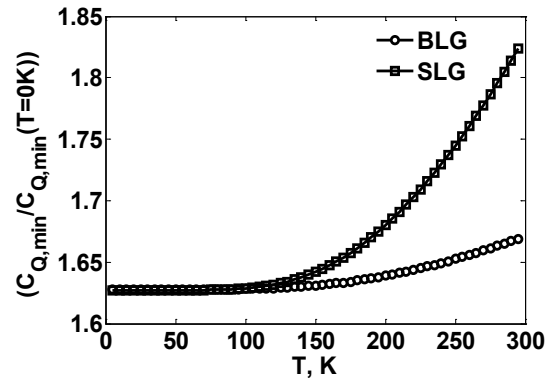

Fig. 3. Dependence of the minimum quantum capacitance on temperature for SLG (squares) and BLG (circles)

4. CONCLUSIONS

In this work, we report an analytical model of the quantum capacitance in single and bilayer graphene which can be used in the accurate modelling of GFET devices as well as in VLSI circuits. The temperature dependence of the quantum capacitance has been examined analytically, by

adopting three temperature values 77 K, 120 K and 300 K. The quantum capacitance of both SLG and BLG has a minimum value at the Dirac point, while the trends increase significantly for BLG, it slightly changes for SLG. The comparison of the simulations to the experimental measurements shows a good agreement which reflects the capability of the model to predict the temperature dependence of the quantum capacitance. Furthermore, a significant similarity was found between SLG and BLG concerning the effect of electron-hole puddles formation in the low-temperature regime.

Acknowledgments

REFERENCES

1. **Novoselov, K.S., Geim, A.K., Morozov, S.V., Jiang, D., Zhang, Y., Dubonos, S.V., Grigorieva, I.V., Firsov, A.A.** Electric Field Effect in Atomically Thin Carbon Films *Science* 306 (5696) 2004: pp. 666 – 669.
https://doi.org/10.1038/nmat3417

2. **Fates, R., Raskin, J.P.** Linear and Non-Linear Electrical Behaviors in Graphene Ribbon Based Devices *Journal of Science: Advanced Materials and Devices* 3 (3) 2018: pp. 366 – 370.
https://doi.org/10.1016/j.jsamd.2018.06.001

3. **Yadav, V.K., Chakraborty, H., Klein, M.L., Waghmare, U.V., Rao, C.** Defect-Enriched Tunability of Electronic and Charge-Carrier Transport Characteristics of 2D Borocarbonitride (BCN) Monolayers from ab Initio Calculations *Nanoscale* 11 (41) 2019: pp. 19398 – 19407.
https://doi.org/10.1039/C9NR04096J

4. **Squires, A., Gao, X., van der Laan, T., Han, Z., Du, J.** Adding a Tuneable Response to a Terahertz Metasurface using a Graphene Thin Film *Journal of Infrared, Millimeter and Terahertz Wave* 43 (9) 2022: pp. 806 – 818.
https://doi.org/10.1007/s10762-022-00883-1

5. **Icking, E., Banszerus, L., Wörtche, F., Volmer, F., Schmidt, P., Steiner, C., Engels, S., Hesselmann, J., Goldsche, M., Watanabe, K.** Transport Spectroscopy of Ultraclean Tunable Band Gaps in Bilayer Graphene *Advanced Electronic Materials* 8 (11) 2022: pp. 2200510.
https://doi.org/10.1002/aelm.202200510

6. **Alattas, M., Schwingenschlögl, U.** Band Gap Control in Bilayer Graphene by Co-Doping with bn Pairs *Scientific Reports* 8 (1) 2018: pp. 17689.
https://doi.org/10.1038/s41598-018-35671-2

7. **Gayduchenko, I., Xu, S., Alymov, G., Moskotin, M., Tretyakov, I., Taniguchi, T., Watanabe, K., Goltsman, G., Geim, A.K., Fedorov, G.** Tunnel Field-Effect Transistors for Sensitive Terahertz Detection *Nature Communications* 12 (1) 2021: pp. 1 – 8.
https://doi.org/10.1038/s41467-020-20721-z

8. **Cao, R., Fan, S., Yin, P., Ma, C., Zeng, Y., Wang, H., Khan, K., Wageh, S., Al-Ghamd, A.A., Tareen, A.K.** Mid-Infrared Optoelectronic Devices Based on Two-Dimensional Materials beyond Graphene: Status and Trends *Nanomaterials* 12 (13) 2022: pp. 2260.
https://doi.org/10.3390/nano12132260

9. **Fates, R., Bouridah, H., Raskin, J.P.** Probing Carrier Concentration in Gated Single, Bi- and Tri-Layer CVD Graphene using Raman Spectroscopy *Carbon* 149 (8) 2019: pp. 390 – 399.
https://doi.org/10.1016/j.carbon.2019.04.078

10. **Cho, S., Fuhrer, M.** Massless and Massive Particle-in-a-Box States in Single-and Bi-Layer Graphene *Nano Research* 4 2011: pp. 385 – 392.
https://doi.org/10.1007/s12274-011-0093-1

11. **Xu, H., Zhang, Z., Wang, Z., Wang, S., Liang, X., Peng, L.M.** Quantum Capacitance Limited Vertical Scaling of Graphene Field-Effect Transistor *American Chemical Society* 5 (3) 2011: pp. 2340 – 2347.
https://doi.org/10.1021/nn200026e

12. **Xu, H., Zhang, Z., Peng, L.M.** Measurements and Microscopic Model of Quantum Capacitance in Graphene *Applied Physics Letters* 98 (13) 2011: pp. 133122.
https://doi.org/10.1063/1.3574011

13. **Cheremisin, M.** Quantum Capacitance of the Monolayer Graphene *Physica E: Low-dimensional Systems and Nanostructures* 69 2015: pp. 153 – 158.
https://doi.org/10.1016/j.physe.2015.01.018

14. **Qiang, X., Guangmin, Y., Xiaofeng, F., Weitao, Z.** Improving the Quantum Capacitance of Graphene-Based Supercapacitors by the Doping and Co-Doping: First-Principles Calculations *American Chemical Society Omega* 4 (8) 2019: pp. 13209 – 13217.
https://doi.org/10.1021/acsomega.9b01359

15. **Yu, G.L., Jalil, R., Belle, B., Mayorov, A.S., Blake, P., Schedin, F., Morozov, S.V., Ponomarenko, L.A., Chiappini, F., Wiedmann, S., Zeitler, U., Katsnelson, M.I., Geim, A.K., Novoselov, K.S. Elias, D. C.** Interaction Phenomena in Graphene Seen Through Quantum Capacitance *Proceedings of the National Academy of Sciences* 110 (9) 2013: pp. 3282 – 3286.
https://doi.org/10.1073/pnas.130059911

16. **Ju, W., Lee, S.** Al Back-Gated Graphene Field-Effect Transistors for Capacitive Sensing Applications Based on Quantum Capacitance Effect *American Institute of Physics Advances* 12 (9) 2022: pp. 095210.
https://doi.org/10.1063/5.0101754

17. **Koshino, M., Tsuneya, A.** Orbital Diamagnetism in Multilayer Graphenes: Systematic Study with the Effective Mass Approximation *Physical Review B* 76 (8) 2007: pp. 085425.
https://doi.org/10.1103/PhysRevB.76.085425

18. **Collins, M.J., Zhang, F., Bojko, R., Chrostowski, L., Rechtsman, M.C.** Integrated Optical Dirac Physics via Inversion Symmetry Breaking *Physical Review A* 94 (6) 2016: pp. 063827.
https://doi.org/10.1103/PhysRevA.94.063827

19. **Aguirre-Morales, J.D., Fregonese, S., Mukherjee, C., Wei, W., Happy, H., Maneux, C., Zimmer, T.** A Large-Signal Monolayer Graphene Field-Effect Transistor Compact Model for RF-Circuit Applications *IEEE Transactions on Electron Devices* 64 (10) 2017: pp. 4302 – 4309.
https://doi.org/10.1109/TED.2017.2736444

20. **Debbarma, R., Nguyen, N.H.L., Berry, V.** Defect Guided Conduction in Graphene-Derivatives and MoS2: Two-Dimensional Nanomaterial Models *Applied Materials Today* 23 2021: pp. 101072.
https://doi.org/10.1016/J.APMT.2021.101072

21. **Aguirre-Morales, J.D., Fregonese, S., Mukherjee, C., Maneux, C., Zimmer, T.** An Accurate Physics-Based Compact Model for Dual-Gate Bilayer Graphene FETs *IEEE*

Transactions on Electron Devices 62 (12) 2015: pp. 4333 – 4339.
https://doi.org/10.1109/TED.2015.2487243

22. **Bera, M., Kharb, R., Sharma, N., Sharma, A., Sehrawat, R., Pandey, S., Mittal, R., Tyagi, D.** Influence of Quantum Capacitance on Charge Carrier Density Estimation in a Nanoscale Field-Effect Transistor with a Channel Based on a Monolayer WSe2 Two-Dimensional Crystal Semiconductor *Journal of Electronic Materials* 48 (6) 2019: pp. 3504 – 3513.
https://doi.org/10.1007/s11664-019-07058-0

23. **Rozhkov, A.V., Sboychakov, A., Rakhmanov, A., Nori, F.** Electronic Properties of Graphene-Based Bilayer Systems *Physics Reports* 648 2016: pp. 1 – 104.
https://doi.org/10.1016/j.physrep.2016.07.003

24. **Fates, R., Remmouche, R., Benkedidah, T., Raskin, J.P.** Evolution of the Raman Spectra Features of Defective Monolayer Graphene in Back-Gate Configuration: Experimental Study *Diamond and Related Materials* 136 (6) 2023: pp. 109919.
https://doi.org/10.1016/j.diamond.2023.109919

25. **Fates, R., Remmouche, R., Benkedidah, T.** Electrical Characteristics of Single Layer Graphene Ribbons in a Wide Temperature Range *Materials Science (Medžiagotyra)* Early access 2023.
https://doi.org/10.5755/j02.ms.33700

26. **Barbier, M., Vasilopoulos, P., Peeters, F.M., Pereira, J.M.** Bilayer Graphene with Single and Multiple Electrostatic Barriers: Band Structure and Transmission *Physical Review B* 79 (15) 2009: pp. 155402.
https://doi.org/10.1103/PhysRevB.79.155402

27. **Khaledian, M., Ismail, R., Saeidmanesh, M., Ahmadi, M., Akbari, E.** Carrier Statistics and Quantum Capacitance Models of Graphene Nanoscroll *Journal of Nanomaterials* 2014: pp. 762143.
https://doi.org/10.1155/2014/762143